

ROTSE-III OBSERVATIONS OF THE EARLY AFTERGLOW FROM GRB 030329

D. A. SMITH,¹ E. S. RYKOFF,¹ C. W. AKERLOF,¹ M. C. ASHLEY,² D. BIZYAEV,^{3,4} T. A. MCKAY,¹ A. MUKADAM,⁵ A. PHILLIPS,²
R. QUIMBY,⁵ B. SCHAEFER,⁵ D. SULLIVAN,⁶ H. F. SWAN,¹ W. T. VESTRAND,⁷ J. C. WHEELER,⁵ AND J. WREN⁷

Received 2003 July 17; accepted 2003 September 4; published 2003 September 30

ABSTRACT

Using two identical telescopes at widely separated longitudes, the ROTSE-III network observed decaying emission from the remarkably bright afterglow of gamma-ray burst GRB 030329. In this report we present observations covering 56% of the period from 1.5 to 47 hr after the burst. We find that the light curve is piecewise consistent with a power-law decay. When the ROTSE-III data are combined with data reported by other groups, there is evidence for five breaks within the first 20 hr after the burst. Between two of those breaks, observations from 15.9 to 17.1 hr after the burst at 1 s time resolution with McDonald Observatory's 2.1 m telescope reveal no evidence for fluctuations or deviations from a simple power law. Multiple breaks may indicate complex structure in the jet. There are also two unambiguous episodes at 23 and 45 hr after the burst in which the intensity becomes consistent with a constant for several hours, perhaps indicating multiple injections of energy into the GRB/afterglow system.

Subject heading: gamma rays: bursts

1. INTRODUCTION

The Robotic Optical Transient Search Experiment (ROTSE) program is dedicated to recording optical observations of gamma-ray bursts (GRBs) within seconds of their detection at high energies. Although the study of late-time afterglows has revolutionized our understanding of GRBs, comparatively little is known about the nature and diversity in the prompt optical and early afterglow emission (Piran 1999). To date, the ROTSE-I observations of GRB 990123 remain the only optical detections of a GRB while the burst was still bright in gamma rays (Akerlof et al. 1999). Rapid observations of many bursts with ROTSE-I and the Livermore Optical Transient Imaging System demonstrate that prompt emission is not, in general, well represented by extrapolation of late-time decay curves (Kehoe et al. 2001; Park et al. 1999). More sensitive instruments are required to study prompt emission from typical bursts.

In preparation for the *High Energy Transient Explorer (HETE-2)*; Vanderspek et al. 1999) and the *Swift* satellites (Gehrels 2000), which can distribute rapid localizations of GRBs with arcminute accuracy, the ROTSE team developed a new set of 0.45 m telescopes. The ROTSE-III instruments use fast optics ($f/1.9$) to yield a $1^{\circ}85 \times 1^{\circ}85$ field of view over a 4 megapixel CCD camera. Four of these robotically controlled automatically scheduled instruments are being erected around

the globe, both to increase the amount of sky available for instant viewing and to enable around-the-clock coverage of GRB afterglow behavior (Akerlof et al. 2003). At the time of this writing, the first two instruments, labeled ROTSE-IIIa and ROTSE-IIIb, are operating at Siding Spring Observatory in New South Wales, Australia, and McDonald Observatory at Ft. Davis, Texas, respectively. The installation of ROTSE-IIIc is nearing completion in Namibia, and ROTSE-IIId is slated to arrive in Turkey in the fall of 2003.

Within a week of the first two ROTSE-III instruments becoming fully operational, the network was tested by the discovery with *HETE-2* of GRB 030329. Spectroscopic observations found the source to lie at a redshift of $z = 0.168$ (Greiner et al. 2003), which makes it the closest GRB to the Earth yet to be measured, with the possible exception of the anomalously faint GRB 980425 (Galama et al. 1999). This event provided the first direct spectral evidence for a supernova associated with a high-redshift GRB (Stanek et al. 2003; Hjorth et al. 2003; Kawabata et al. 2003). We report here on the light curve of GRB 030329 for the first 2 days of observations by ROTSE-IIIa and IIIb.

2. OBSERVATIONS AND ANALYSIS

GRB 030329 was first observed by the instruments on board the *HETE-2* satellite at 11:37:14.67 UTC. Ground analysis of the Soft X-Ray Camera data produced a localization that was reported in a Gamma-Ray Burst Coordinate Network (GCN) Notice 73 minutes after the burst (Vanderspek et al. 2003). Although the burst's celestial location was above the Australian horizon at the time, the ROTSE-IIIa connection to the GCN was temporarily experiencing sporadic outages. It was therefore impossible for the ROTSE automated scheduler daemon to respond to the alert. However, electronic mail was also distributed to ROTSE team members, and a manual response by the ROTSE-IIIa telescope was initiated over the Internet within 15 minutes of the alert's distribution, 88 minutes after the burst itself.

Clouds and intermittent rain interfered with observations and delayed analysis of the images, but once Peterson & Price (2003) and Torii (2003) identified the optical counterpart, we were able to extract a light curve from the setting source. Our earliest useful images began 92 minutes after the burst event

¹ University of Michigan at Ann Arbor, Department of Physics, 2477 Randall Laboratory, 500 East University Avenue, Ann Arbor, MI 48104; donaldas@umich.edu, erykoff@umich.edu, akerlof@umich.edu, tamckay@umich.edu, hflewell@umich.edu.

² School of Physics, Department of Astrophysics and Optics, University of New South Wales, Kensington Campus, Old Main Building, Kensington, Sydney NSW 2052, Australia; mcba@phys.unsw.edu.au, a.phillips@unsw.edu.au.

³ Department of Physics, University of Texas at El Paso, Physical Science Building 210, 500 West University Avenue, El Paso, TX 79968; dmbiz@baade.physics.utep.edu.

⁴ Sternberg Astronomical Institute, 119992, Universitetski Pr., 13, Moscow, Russia.

⁵ Department of Astronomy, University of Texas at Austin, 1 University Station, C1400, Austin, TX 78712; anjum@astro.as.utexas.edu, quimby@astro.as.utexas.edu, schaefer@astro.as.utexas.edu, wheel@hej3.as.utexas.edu.

⁶ School of Chemical and Physical Sciences, Victoria University of Wellington, P.O. Box 600, Wellington, NZ; denis.sullivan@vuw.ac.nz.

⁷ Los Alamos National Laboratory, NIS-2 MS D436, Los Alamos, NM 87545; vestrand@lanl.gov, jwren@nis.lanl.gov.

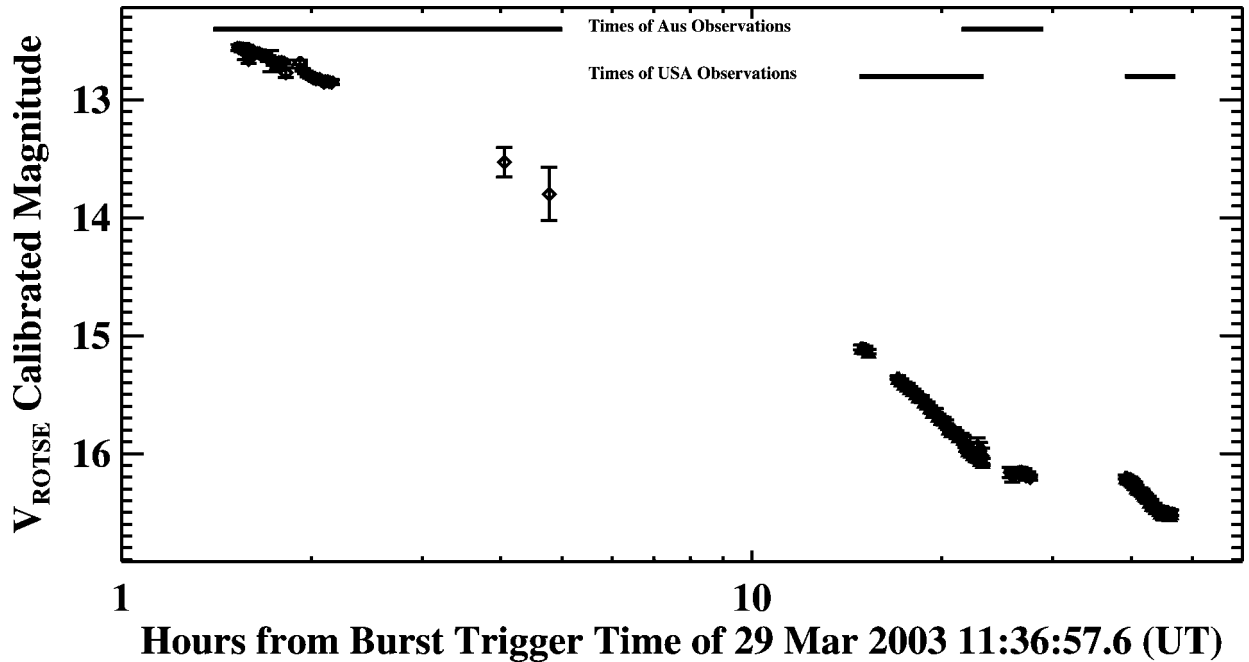


FIG. 1.—Decay of GRB 030329 over the first 2 days of observations. Magnitudes are calibrated to V_{ROTSE} as described in the text. Diamonds indicate measurements made with ROTSE-IIIa and triangles those made with ROTSE-IIIb. Intervals when the source was above the horizon at each site are indicated by horizontal bars at the top of the graph.

(Rykoff & Smith 2003). At 4.8 hr after the burst, the air mass to the source grew too large for further observation.

ROTSE-IIIb (in Texas) began observations 14.8 hr after the burst and followed the source for a further 8.5 hr. Once the source had risen again in Australia, contemporaneous observation from both ROTSE-III instruments was possible for 1.8 hr. The ROTSE-III automatic scheduler normally plans observations of fading GRB afterglows to occur at logarithmically increasing intervals, leading to gaps in coverage at the start of each night’s observing. As it became clear how bright this source was, we overrode the default schedule to instruct the instruments to look at nothing else as long as GRB 030329 was above the local horizon.

The ROTSE-III images were bias-subtracted and flat-fielded in the standard way. For images recorded later than 10 hr after the burst, we co-added sets of 10 frames before deriving a light curve. We applied SExtractor (Bertin & Arnouts 1996) with aperture photometry to these co-added images to detect objects and derive their intensities. We compared these intensities to the USNO-A2.0 catalog to derive an approximate R -band magnitude zero-point offset for the field. Zero-point offsets among the ROTSE images are determined through application of a relative photometry procedure. Absolute calibration to a V -magnitude equivalent (dubbed V_{ROTSE}) is derived by comparison of several nearby stable stars to the $UBVR_cI_c$ photometry of Henden (2003).

The offset between unfiltered V_{ROTSE} observations and standard V magnitudes is a function of color. Without color information for the early-time afterglow, we have not applied any color correction to these data. However, from 6.0 to 14.4 hr after the burst, during observations reported by Burenin et al. (2003b), the afterglow color is rather blue, with $V-R \approx 0.3$. This color remained stable through a break in the light curve. If the afterglow maintained this color throughout the ROTSE-III observations, it would be appropriate to further adjust the V_{ROTSE} magnitudes reported here to be approximately 0.5 mag brighter.

GRB 030329 was also observed with a time resolution of 1 s using a CCD time-series photometer mounted at the prime focus position of the McDonald Observatory 2.1 m telescope. The photometer “Argos” (R. Nathem & A. Mukadam 2003, in preparation) operates in frame transfer mode and thus allows rapid exposures as short as 1 s. The time-series photometry started 15.87 hr after the burst trigger and continued for 4290 s in essentially photometric conditions. No filter was used, so the spectral response of the instrument was dominated by the combination of a typical CCD sensitivity and the Earth’s atmosphere: the transmission is about 70% in the wavelength range 560–640 nm and greater than 50% in the wavelength range 450–800 nm.

Typical ADU count rates for the optical transient were $17,000 \text{ s}^{-1}$, while the sky contributed about $10,500 \text{ counts s}^{-1}$ in the chosen software aperture. There were two comparison stars in the $2'.8$ field of view of the instrument, and sky-subtracted light curves for each object were obtained by using an optimized circular software aperture. A corrected light curve for the target object was then generated by dividing its light curve to the sum of the two comparison star light curves (which have been normalized to unity).

3. RESULTS

The full light curve from both ROTSE-IIIa and IIIb is shown on a logarithmic scale in the top panel of Figure 1. Figure 2 shows two segments of the light curve on expanded scales. In this section, we describe the behavior of the afterglow during each observing sequence.

The poor observing conditions during the first observing run (from 1.5 to 4.8 hr after the burst) introduce large systematic errors into the photometry, but there is no evidence for any significant deviations from a power-law decay with an index of 0.88 ± 0.05 , a value not atypical for early GRB afterglows. The earliest detections reveal an unfiltered V_{ROTSE} magnitude

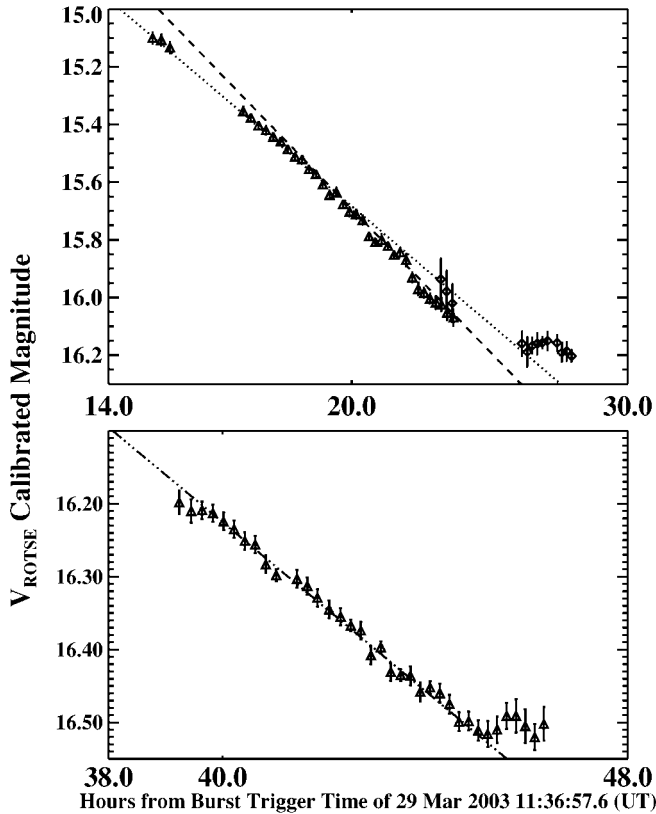


FIG. 2.—Expanded views of two segments of the ROTSE-III light curve for GRB 030329. Diamonds indicate measurements made with ROTSE-IIIa and triangles those made with ROTSE-IIIb. *Top*: The interval from 14 to 30 hr after the burst; *bottom*: the time from 38 to 48 hr. These panels also overlay best-fit power-law functions onto the observations. The data in the top panel are clearly inconsistent with a single power-law decay. Parameters for these functions are given in Table 1. The burst intensity levels off at ~ 23 hr after the burst, maintaining a constant intensity for the rest of the Australian night, but begins decaying again in the second night of Texas observations, as shown in the bottom panel, before entering a second flattening episode.

of 12.55, over 100 times brighter than any other afterglow to date to be observed at this epoch (Price et al. 2003), consistent with the very low redshift for the object. The latest points in this sequence, recorded after an hour during which ROTSE-IIIa automatically ceased operation because of a light rain, are also consistent with the same decay curve.

When ROTSE-IIIb commenced observations at 14.8 hr, the intensity of GRB 030329 was decaying much more rapidly, consistent with a power-law index of 1.85 ± 0.07 and strongly inconsistent with the earlier curve observed with ROTSE-IIIa. If we assume a single sharp transition from one decay mode to the other, these data predict a transition time of ~ 12 – 14 hr after the burst. Over the course of the 8.5 hr observing sequence with ROTSE-IIIb on 2003 March 30, the decay slope steepened further, demanding the introduction of a third power law with decay index of 2.25 ± 0.08 . The best-fit transition time to this decay slope is at 19.0 hr after the burst.

The interval during which GRB 030329 was observed by the 2.1 m coincided with the early part of this decay phase, before the break at 19 hr. The corrected light curve at 1 s resolution shows the optical transient to be fading smoothly. The fitted power-law decline has an index of 1.98 ± 0.02 . This power law fits well to both the beginning and the ending 500 s time intervals with the same normalization to within 0.2%, thus indicating that there were no departures from the overall power-law de-

TABLE 1
PARAMETERS OF BEST-FIT POWER-LAW
DECAY CURVE

Start Time (hr)	Stop Time (hr)	Index
1.5	4.8	0.87 ± 0.03
14.8	19.0	1.85 ± 0.06
19.0	23.0	2.25 ± 0.08
23.0	26.0	<0.4
39.5	45.0	2.34 ± 0.08
45.0	46.5	<0.4

cline. The largest deviation from the best-fit power law was one point that was low by only 4.4σ . Analysis of binned light curves reveals no significant fluctuations from the power law on any longer timescales. The computed discrete Fourier transform did not reveal any power out to the Nyquist frequency of 0.5 Hz up to a limit of 2 mmag (i.e., 0.2% change in intensity). In all, we found no deviations from a simple power-law decline.

During the interval when both ROTSE-III instruments could observe the source simultaneously, our calibration procedure yielded consistent results. However, ROTSE-IIIa subsequently observed the source intensity to level off and remain constant for at least 3 hr. When the source again became visible to ROTSE-IIIb in Texas, it was found to still have the same intensity as when last seen by ROTSE-IIIa. It shortly commenced a rapid decay phase, consistent with a single power law of index 2.34 ± 0.08 . This decay rate is consistent with the decay slope observed at the end of the previous night. The decay phase lasted for approximately 6 hr. The source then entered a second flattening phase that was still continuing when observations ceased for the night 2 hr later.⁸

The decay curve for GRB 030329 over its first 2 days is clearly inconsistent with a single power-law function. We find that at least four power laws plus two intervals of constant intensity are necessary to adequately reproduce the behavior of the light curve. Three of these functions are plotted as dashed lines in Figure 2. The decay indices as well as the intervals over which each power-law segment applies are given in Table 1.

4. DISCUSSION

The worldwide distribution of the ROTSE-III network allows for unprecedented coverage of the early decay curve of GRB afterglows, and in the case of GRB 030329, the afterglow was above the horizon for 56% of the first 47 hr after the event. Since the ROTSE-III network was only half complete at the time of GRB 030329, there are still large gaps in the derived light curve when the source was not visible to either telescope. However, at least two groups have published observations of the afterglow's behavior during the time on the first day when neither ROTSE-IIIa nor ROTSE-IIIb could observe it (Burenin et al. 2003a; Oksanen, Henriksson, & Tuukkanen 2003; Lipunov et al. 2003; Kindt, Andersen, & Jakobsen 2003).

Uemura et al. (2003) observed GRB 030329 with a variety of telescopes from 1.2 to ~ 14 hr after the event, and they report three breaks in the light curve during this time: from 0.74 ± 0.02 to 0.95 ± 0.01 at $t = 2.04$ hr, to 0.65 ± 0.04 at $t = 3.9$ hr, and again to 1.16 ± 0.01 at $t = 5.4$ hr. This characterization is consistent with the ROTSE-IIIa data, which have neither sufficient coverage nor small enough errors to distin-

⁸ The ROTSE-III light curve is stored in electronic form at <http://www.rotse.net/transients/grb030329>.

guish between this and the best-fit single power law reported in § 3. Burenin et al. (2003b) present observations taken with the 1.5 m Russian-Turkish Telescope shortly after the time of this last transition and give a slope of 1.19 ± 0.01 from 6.2 to 14.4 hr after the burst, after which the slope changes to ~ 1.9 , which is consistent with the ROTSE-IIIb observations at 14.8 hr. The Japanese and Turkish programs, therefore, neatly fill in the gap between ROTSE-III observations, and the joint data set provides evidence for five changes in slope decay index within the first 20 hr after the burst.

No GRB afterglow has been observed nearly as intensely as GRB 030329, and for most other bursts only a single steepening in the light-curve decay has been reported. These breaks have been taken as evidence for deceleration of a relativistic jet: as the jet decelerates, the beaming angle must increase, and when the beaming angle exceeds the jet angle, the intensity of visible light is expected to decrease more rapidly (Rhoads 1997; Sari, Piran, & Halpern 1999; Perna, Sari, & Frail 2003). Multiple breaks within a single decay curve are more difficult to interpret in this paradigm, but Wei & Jin (2003), for example, have suggested that they may result from off-axis viewing geometry or perhaps nonuniform structure within the jet. A detailed analysis of what geometry five decay breaks might demand is beyond the scope of this Letter, but the data clearly are not consistent with the simplest models and demand caution when trying to interpret $t \sim 0.5$ days as *the* jet break (Granot, Nakar, & Piran 2003; Burenin et al. 2003b; Price et al. 2003).

The other striking feature of the afterglow is the deviation from its rapid decay, beginning at ~ 23 hr after the burst. In

the ROTSE-III observations, the intensity levels off and remains constant for several hours. A second decay phase begins ~ 39 hr after the burst. It is unlikely that this episode is related to the emergence of a supernova in the light curve, as the first spectral evidence for a supernova associated with GRB 030329 emerged only after ~ 7 days (Stanek et al. 2003). At 1 day after the event, the optical intensity should be dominated by the burst afterglow. Furthermore, the light curve flattens yet again at ~ 44 hr. Wei & Jin (2003) argue that geometric factors could produce a flattening of the light curve at about this time, but it is hard to understand the repeating nature of the phenomenon within that paradigm. On the other hand, Granot et al. (2003) have interpreted these episodes as refreshed shocks produced by further ejection events from the central engine catching up with the decelerating blast wave. In this interpretation, the central engine remains an active part of the GRB process well into the afterglow phase, further underscoring the need for early and thorough observations of the entire burst event if the complex physical interactions are ever to be teased out.

This work has been supported by NASA grants NAG5-5281 and F006794, NSF grant AST 01-19685, the Michigan Space Grant Consortium, the Australian Research Council, the University of New South Wales, the University of Texas, and the University of Michigan. D. A. S. is supported by an NSF Astronomy and Astrophysics Postdoctoral Fellowship under award AST 01-05221. Work performed at LANL is supported by NASA SR&T through Department of Energy contract W-7405-ENG-36 and through internal LDRD funding.

REFERENCES

- Akerlof, C., et al. 1999, *Nature*, 398, 400
 ———. 2003, *PASP*, 115, 132
 Bertin, E., & Arnouts, S. 1996, *A&AS*, 117, 393
 Burenin, R., et al. 2003a, *GCN Circ.* 2001 (<http://gcn.gsfc.nasa.gov/gcn/gcn3/2001.gcn3>)
 ———. 2003b, *Astron. Lett.*, 29(9), 573
 Galama, T. J., et al. 1999, *A&AS*, 138, 465
 Gehrels, N. A. 2000, *Proc. SPIE*, 4140, 42
 Granot, J., Nakar, E., & Piran, T. 2003, preprint (astro-ph/0304563)
 Greiner, J., et al. 2003, *GCN Circ.* 2020 (<http://gcn.gsfc.nasa.gov/gcn/gcn3/2020.gcn3>)
 Henden, A. 2003, *GCN Circ.* 2023 (<http://gcn.gsfc.nasa.gov/gcn/gcn3/2023.gcn3>)
 Hjorth, J., et al. 2003, *Nature*, 423, 847
 Kawabata, K. S., et al. 2003, *ApJ*, 593, L19
 Kehoe, R., et al. 2001, *ApJ*, 554, L159
 Kindt, L., Andersen, H.-H., & Jakobsen, A. 2003, *GCN Circ.* 2193 (<http://gcn.gsfc.nasa.gov/gcn/gcn3/2193.gcn3>)
 Lipunov, V., et al. 2003, *GCN Circ.* 2091 (<http://gcn.gsfc.nasa.gov/gcn/gcn3/2091.gcn3>)
 Oksanen, A., Henriksson, R., & Tuukkanen, M. 2003, *GCN Circ.* 2010 (<http://gcn.gsfc.nasa.gov/gcn/gcn3/2010.gcn3>)
 Park, H. S., et al. 1999, *A&AS*, 138, 577
 Perna, R., Sari, R., & Frail, D. 2003, *ApJ*, 594, 397
 Peterson, B., & Price, P. 2003, *GCN Circ.* 1985 (<http://gcn.gsfc.nasa.gov/gcn/gcn3/1985.gcn3>)
 Piran, T. 1999, *Phys. Rep.*, 314(6), 575
 Price, P., et al. 2003, *Nature*, 423, 844
 Rhoads, J. E. 1997, *ApJ*, 487, L1
 Rykoff, E. S., & Smith, D. A. 2003, *GCN Circ.* 1995 (<http://gcn.gsfc.nasa.gov/gcn/gcn3/1995.gcn3>)
 Sari, R., Piran, T., & Halpern, J. P. 1999, *ApJ*, 519, L17
 Stanek, K. Z., et al. 2003, *ApJ*, 591, L17
 Torii, K. 2003, *GCN Circ.* 1986 (<http://gcn.gsfc.nasa.gov/gcn/gcn3/1986.gcn3>)
 Uemura, M., et al. 2003, *Nature*, 423, 843
 Vanderspek, R., Villaseñor, J., Doty, J., Jernigan, J. G., Levine, A., Monnelly, G., & Ricker, G. R. 1999, *A&AS*, 138, 565
 Vanderspek, R., et al. 2003, *GCN Circ.* 1997 (<http://gcn.gsfc.nasa.gov/gcn/gcn3/1997.gcn3>)
 Wei, D. M., & Jin, Z. P. 2003, *A&A*, 400, 415